Pharm Res (2013) 30:3214–3224
DOI 10.1007/s11095-013-1230-1

RESEARCH PAPER

# Binary Blend of Glyceryl Monooleate and Glyceryl Monostearate for Magnetically Induced Thermo-Responsive Local Drug Delivery System

Abebe E. Mengesha • Robert J. Wydra • J. Zach Hilt • Paul M. Bummer

Received: 5 December 2012 / Accepted: 14 October 2013 / Published online: 25 October 2013


## ABSTRACT

***Purpose*** To develop a novel monoglycerides-based thermal-sensitive drug delivery system, specifically for local intracavitary chemotherapy.

***Methods*** Lipid matrices containing mixtures of glyceryl monooleate (GMO) and glyceryl monostearate (GMS) were evaluated for their potential application as magnetically induced thermo-responsive local drug delivery systems using a poorly water-soluble model drug, nifedipine (NF). Oleic acid-modified iron oxide (OA-$Fe_3O_4$) nanoparticles were embedded into the GMO-GMS matrix for remote activation of the drug release using an alternating magnetic field (AMF).

***Results*** The crystallization behavior of binary blends of GMO and GMS as characterized by DSC did show temperature dependent phase transition. GMO-GMS (75:25 wt%) blend showed a melting ($T_m$) and crystallization ($T_c$) points at 42°C and 37°C, respectively indicating the potential of the matrix to act as an '*on-demand*' drug release. The matrix released only 35% of the loaded drug slowly in 10 days at 37°C whereas 96% release was obtained at 42°C. A concentration of 0.5% OA-$Fe_3O_4$ heated the matrix to 42.3 and 45.5°C within 5 min and 10 min of AMF exposure, respectively.

***Conclusions*** The *in vitro* NF release profiles form the monoglycerides matrix containing 0.5% OA-$Fe_3O_4$ nanoparticles after AMF activation confirmed the thermo-responsive nature of the matrix that could provide pulsatile drug release '*on-demand*'.

**KEY WORDS** local drug delivery · monoolein · monostearin · oleic acid-modified iron oxide nanoparticles · thermo-responsive monoglycerides

## ABBREVIATIONS

| | |
|---|---|
| AMF | Alternating magnetic field |
| DSC | Differential scanning calorimetry |
| GMO | Glyceryl monooleate |
| GMS | Glyceryl monostearate |
| NF | Nifedipine |
| OA-$Fe_3O_4$ | Oleic acid-modified iron oxide nanoparticles |
| $T_c$ | Crystallization temperature |
| $T_m$ | Melting temperature |

## INTRODUCTION

It is well recognized that precise spatial and temporal delivery of therapeutic agents to the target site is a means by which maximum effectiveness and safety of the therapy can be realized. Drug delivery triggered by factors, such as pH (1–3), heat (4), magnetic field (5–9), ultrasound (10,11) or combination of two or more stimuli (12), has been studied as a means to increase the drug concentration at the target location, lower systemic toxicity, and provide temporal control over drug release.

Many stimuli-responsive drug delivery systems have been designed and fabricated using polymers (9,13,14). Issues related to polydispersity, kinetic reproducibility, and toxicity imparted by stimuli-responsive functional groups can limit *in vivo* utility (15) of polymer systems.

**Electronic supplementary material** The online version of this article (doi:10.1007/s11095-013-1230-1) contains supplementary material, which is available to authorized users.

A. E. Mengesha
College of Pharmacy & Health Sciences, Drake University
Des Moines, Iowa 50311, USA

R. J. Wydra • J. Z. Hilt
Department of Chemical & Materials Engineering, University of Kentucky, Lexington, Kentucky 40506, USA

P. M. Bummer (✉)
Department of Pharmaceutical Sciences, College of Pharmacy
University of Kentucky, Lexington, Kentucky 40536, USA
e-mail: pbumm01@email.uky.edu

Lipid mixtures provide an alternative platform for stimuli-responsive drug delivery systems (16,17). Many lipids and lipid-based formulations are known to be nontoxic and biocompatible and to enhance the solubility and permeability of many drugs (18,19).

Monoglycerides, such as glyceryl monooleate (GMO) and glyceryl monostearate (GMS), are self-assembling amphiphilic molecules that form a variety of crystalline structures (20) with useful mechanical properties of special interest in drug delivery (16). It is well known that monoglycerides exhibit complex solid-state behavior including melting, crystallization and physical modifications during processing and storage (21). Since the polymorphic behavior is typically monotropic, each polymorph possesses a unique melting point and undergoes transitions at well-defined temperatures (22). The melting and crystallization pattern of a matrix of mixed monoglyceride polymorphs is known to be a function of the composition and can be systematically tuned to achieve desirable properties.

The principle of modifying the physical property of lipid-matrix through blending of components is widely used in the food industry. One example is the utilization of the gel phase properties of long-chain saturated monoglycerides to achieve the structuring of edible oils without addition of high melting point saturated or *trans* fats (23).

The hypothesis of this project is that an appropriate blend of GMO and GMS will provide a thermo-responsive gel matrix that melts at 42°C and solidifies at 37°C. A potential clinical application of a thermo-responsive GMO-GMS gel matrix via an alternating magnetic field (AMF) would be as a drug depot in the treatment of malignant brain tumors. (24). It is envisioned that the gel matrix would be inserted in the cavity remaining after surgical resection of the tumor. It is hypothesized that drug release from this matrix will be strongly temperature-dependent, being rapid at 42°C and ceasing at 37°C. To provide a means of localized heating through the external application of an alternating magnetic field (AMF), oleic acid-modified iron oxide (OA-$Fe_3O_4$) nanoparticles were incorporated into the chosen GMO-GMS matrix. In this study it is demonstrated for the first time that the GMO-GMS matrix, combined with magnetite nanoparticles and subjected to an AMF, exhibited unique properties suitable as a tunable thermo-sensitive local drug delivery system.

## MATERIALS AND METHODS

### Chemicals

1-Oleoyl-rac-glycerol (c18:1, 99%) and 1-monostearoyl-rac-glycerol (c18:0, 99.7%) were purchased form Sigma Aldrich. Nifedipine (NF) and the salts for artificial cerebrospinal fluid (ACSF) were obtained from Fisher Scientific, and used as received. Iron (III) chloride hexahydrate ($FeCl_3 \cdot 6H_2O$), iron (II) chloride tetrahydrate ($FeCl_2 \cdot 4H_2O$), and oleic acid (OA) were obtained from Sigma Aldrich, and used as received. All other chemicals were of analytical purity. Spherical iron-oxide nanoparticles ($Fe_3O_4$, magnetite) with a mean diameter of 20–30 nm were purchased from Nanostructured and Amorphous Materials, Inc.

### Preparation of the Monoglycerides Matrix

Various compositions between 0 and 100 w/w% of GMO-GMS mixtures were prepared by a fusion method. The mixtures were homogenized by repeating a process of melting in water bath at 80°C, shaking, followed by chilling in ice-bath 4–5 times. The samples were characterized using differential scanning calorimetry (DSC). Selected GMO-GMS lipid matrices (25:75, 50:50 and 75:25 wt%) were loaded with 0.25–1.3% oleic acid-modified magnetite (OA-$Fe_3O_4$) nanoparticles for the remote heating using alternating magnetic field (AMF). The *in vitro* release of the model drug nifedipine from the GMO-GMS matrices was studied at 37°C and 42°C in artificial cerebrospinal fluid (ACSF). The AMF-induced pulsatile release profile of NF from GMO-GMS matrix containing 0.5% w/w OA-$Fe_3O_4$ was evaluated.

### Characterization of the Monoglycerides Matrix by Differential Scanning Calorimetry

The thermal behavior and phase diagrams of GMO-GMS systems were investigated using a differential scanning calorimeter (DSC-2920, TA Instruments). The samples were accurately weighed and heated in hermetically sealed aluminum pan at a rate of 5°C/min first from −30°C to 90°C, cooled back to −10°C and then re-heated. The thermograms were analyzed by the resident software for the peak melting temperature ($T_m$) and the peak crystallization temperature ($T_c$) during the first heating cycle and the second melting temperature ($Tm_2$) obtained during the re-heating.

### Synthesis and Characterization of OA-modified $Fe_3O_4$ Nanoparticles

A one-pot co-precipitation method was used to prepare the oleic acid coated iron oxide nanoparticles as previously reported (25). Briefly, aqueous solutions of $FeCl_3 \cdot 6H_2O$ and $FeCl_2.4H_2O$ were combined in a 2:1 molar ratio in a sealed three-neck flask under vigorous stirring and an inert $N_2$ environment. Once 85°C was reached, 5 mL of $NH_4OH$ was injected into the vessel followed by 2 ml of oleic acid and the reaction was carried out for 1 h. The particles were

washed and retrieved with magnetic decanting. Following the wash the particles were dried and stored under vacuum.

### Quantification of Remote Heating

To measure the heating that occurs due to the OA-$Fe_3O_4$ nanoparticles, GMO-GMS matrices containing 0.25–1.3% nanoparticles were exposed to an alternating electromagnetic field (AMF) induced by a custom-built Taylor Winfield induction power supply (model MMF-3-135/400-2) equipped with a solenoid with a 20 mm diameter and five turns. Samples of the matrix were placed in a tube that is placed in the center of the solenoid (Fig. 1). The AMF was applied for 10 min at field strength of 57.0 kA/m and 300 kHz frequency and the temperature was continuously measured by a fluoroptic thermometer from LumaSense Technologies.

### Preparation of Nifedipine Monoglycerides Matrix

GMO-GMS matrix containing 5% w/w nifedipine was prepared using a fusion method. The required amount of nifedipine was first dissolved in molten GMO at 40°C and the solution was added into GMS that previously melted and kept at 65°C. The OA-$Fe_3O_4$ nanoparticles were dispersed into the mixture and cooled while mixing continuously.

### *In Vitro* Release of Nifedipine

The release studies of nifedipine from the mixed monoglyceride matrices were conducted using cellulose ester dialysis tubing (Spectra/Pro® CE Float-A-Lyzer® G2, Spectrum, 1-mL, MWCO 3500–5000 Da, surface area approximately 7.8 $cm^2$) at 37°C and 42°C in artificial cerebrospinal fluid (ACSF) at pH of 7.4 ($n=3$). ACSF contained sodium chloride (124 mM), potassium chloride (1.75 mM), magnesium sulfate (1.3 mM), calcium chloride (2.4 mM), potassium dihydrogen phosphate (1.25 mM), sodium bicarbonate (26 mM) and dextrose (10 mM). One milliliter of freshly prepared nifedipine monoglycerides matrix (equivalent to 0.5 mg nifedipine) was placed into a 1 mL dialysis bag. The dialysis bags were placed in 200 mL ACSF release medium maintained at 37°C or 42°C. Sink condition was maintained throughout the release studies. At selected time intervals, a 1 mL sample of media was withdrawn and replaced with fresh ACSF. The nifedipine content was quantified using a Waters 2629 HPLC system with a Supelco, ABZ+, 5 µm, 4.6×250 mm column and detected at 236 nm. Acetonitrile/water (50:50%v/v) was used as the mobile phase at a flow rate of 1.0 mL/min. Preliminary experiments were conducted to observed the rate at which drug appeared in the receiver compartment when drug in ACSF was placed in the donor compartment.

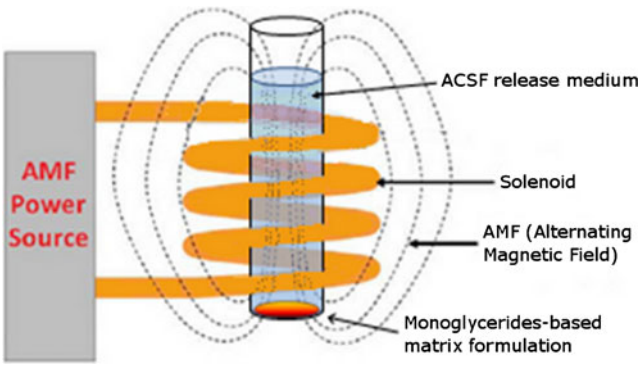


**Fig. 1** Schematic presentation of the heating of the monoglycerides-matrix using AFM. The tube containing the formulation and the ASCF release medium was placed inside the coil.

### AMF-Triggered Release of Nifedipine

The AMF-triggered pulsatile release of nifedipine from the GMO-GMS (75:25% w/w) matrix containing 0.5% OA-$Fe_3O_4$ nanoparticles was studied. The experimental AMF device is shown in Fig. 1. Samples of the matrix (equivalent to 25 µg nifedipine) were placed in centrifuge tube containing 10 mL ACSF at 37°C bath. Every 24 h, the samples were exposed to AMF for 5 min. Two hours prior to AMF exposure, and 2 h following exposure, 0.5 mL of media was withdrawn for HPLC analysis of nifedipine. Fresh ACSF at 37°C was used to replace the volume of media removed.

## RESULTS

A thermo-sensitive matrix offers enormous potential as an 'on demand' drug delivery system where the release of drug could be triggered by external heating. The core hypothesis of this work is that pure monoglycerides undergo phase transitions at well-defined temperatures based on their structure (22) and these transitions may be exploited to formulate a thermo-responsive local drug delivery system. The proposed concept of monoglycerides-based thermo-responsive drug delivery system is schematically illustrated in Fig. 2. When the environmental temperature is 37°C and the lipid chains are in a crystalline state, release of solute drug is significantly slower than when lipid chains melt at 42°C. To identify those systems with the target thermal and drug release properties, binary mixtures of GMO and GMS were evaluated.

### Phase Behavior of GMO-GMS Binary Mixtures

Polymorphism is a common phenomenon in long-chain compounds including fats and lipids (19). Long-chain saturated monoglycerides possess complex polymorphic forms; for GMS these are identified as the stable β-form and

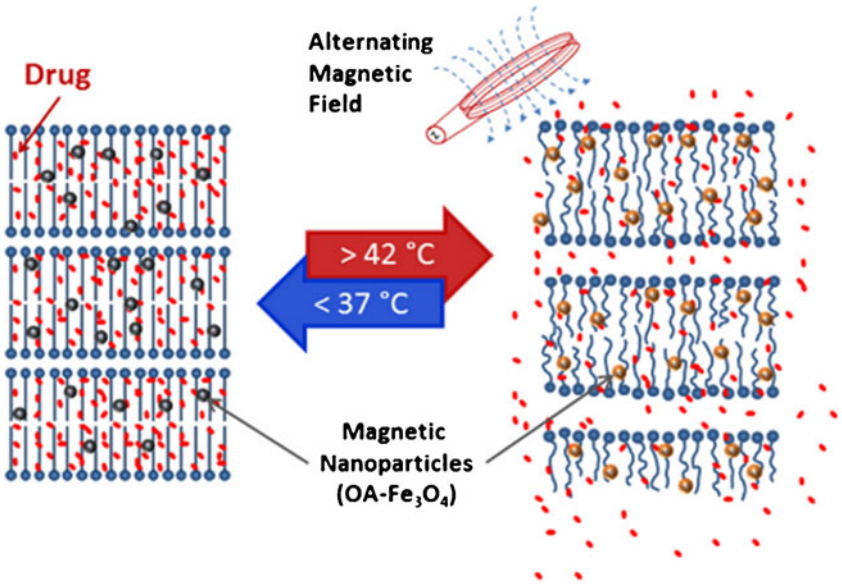


**Fig. 2** Schematic illustration of the proposed concept of monoglycerides-based thermo-responsive drug delivery system. Model on the GMO-GMS matrix containing the OA-$Fe_3O_4$ nanoparticles.

a series of metastable (α, sub-α1 and sub-α2) forms. Unsaturated monoglycerides, like GMO, show a less complex behavior with the occurrence of only one polymorph (26). Blending of saturated and unsaturated monoglycerides is expected to produce complex crystalline behavior.

The phase behavior of GMO-GMS binary mixtures was studied by differential scanning calorimetry (DSC). Presented in Fig. 3 is the thermogram of the 50:50 wt% system of GMO-GMS. Two endothermic melting $T_m$ values were observed, suggesting a GMO-rich phase and a GMS-rich phase co-existing in the gel. While pure GMO has a $T_m$ of 36.8°C (Table I), in the presence of GMS, the GMO-rich phase exhibited a $T_m$ of 38°C. Alternately, for pure GMS, a $T_m$ of 82.7°C was observed (Table I), while in the GMS-rich phase, the $T_m$ dropped to 71.8°C. The $T_m$ values for the GMO-rich and GMS-rich phases as a function of composition are shown in Table I. Increasing the GMO content of the system resulted in a decrease in the $T_m$ of the β-form of the GMS-rich phase by more than 30°C. On the other hand, the $T_m$ of the GMO-rich phase was found to be maximal around 75:25 wt%

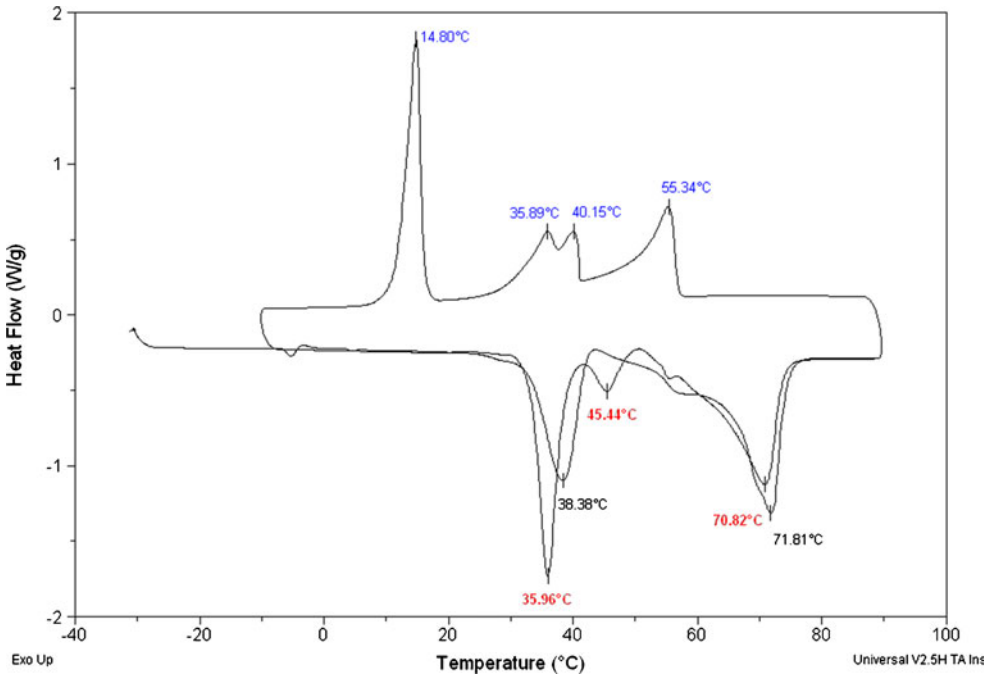


**Fig. 3** DSC thermogram of GMO-GMS (50:50 wt%) matrix, first heating, cooling back and reheating.

**Table I** Phase Behavior of GMO-GMS Binary Mixture

| GMO-GMS (wt%) | Peak $T_m$ | | | Peak $T_c$ | | | | Peak $T_{m2}$ (second melting) | | |
|---|---|---|---|---|---|---|---|---|---|---|
| | GMS-rich phase | New peak | GMO-rich phase | GMS-rich phase | | | GMO-rich phase | GMS-rich phase | | GMO-rich phase |
| | | | | α-form | sub-α1 | sub-α2 | | α-form | sub-α | |
| 0 | 82.7 | – | NA | 71.9 | 47.1 | 41.8 | – | 75.3 | 52.1 | – |
| 11.4 | 80.0 | 51.0 | 33.6 | 68.3 | 45.7 | 40.3 | 11.7 | 78.8 | 50.2 | 34.3 |
| 21.8 | 78.4 | 49.2 | 34.3 | 65.5 | 44.2 | 38.9 | 13.1 | 76.8 | 48.5 | 34.3 |
| 31.6 | 76.6 | 48.1 | 36.4 | 63.3 | 43.2 | 38.1 | 13.5 | 75.8 | 47.3 | 34.6 |
| 37.6 | 74.5 | 46.7 | 36.8 | 59.9 | 42.0 | 36.7 | 13.5 | 73.1 | 45.7 | 34.8 |
| 49.6 | 71.8 | 45.1 | 38.0 | 55.5 | 40.5 | 35.5 | 14.2 | 70.7 | 44.6 | 35.2 |
| 59.9 | 68.3 | 42.9 | 38.8 | 50.9 | 39.1 | 34.2 | 13.6 | 67.9 | 43.5 | 35.4 |
| 70.0 | 60.4 | – | 41.5 | 44.1 | 37.1 | 32.8 | 14.1 | 63.8 | – | 35.8 |
| 75.0 | 55.7 | – | 42.4 | 37.8 | – | 30.7 | 15.0 | 60.5 | – | 38.6 |
| 79.8 | 52.9 | – | 40.5 | 36.4 | – | – | 15.0 | 57.5 | – | 35.7 |
| 89.6 | 46.9 | – | 37.1 | 20.7 | – | – | 13.5 | – | – | 35.3 |
| 100 | NA | – | 36.8 | – | – | – | 6.8 | – | – | 35.0 |

Values are average of two measurements

GMO-GMS (Fig. 4). Of interest to this study is the observation that the $T_m$ of the GMO-rich phase (42.4°C) was found to be very close to the target value for application in a remotely-heated matrix. As the system concentration of GMO decreased further, the $T_m$ of the GMO-phase decreased only slightly. Upon cooling the 75:25 wt% GMO-GMS matrix, the crystallization temperature, $T_c$, of 37.8°C is also very close to the target value for application to a remote-heated matrix. Appearance of new peaks in the DSC thermogram of 10–60% GMO in GMS blends (Table I) may indicate the formation of new molecular rearrangements of the monoglycerides. Figure 5 shows the phase diagram of the binary blend of GMO and GMS based on the peak melting temperature ($T_m$).

In applying a thermo-sensitive delivery system, it is anticipated that *in vivo* the drug-containing matrix will

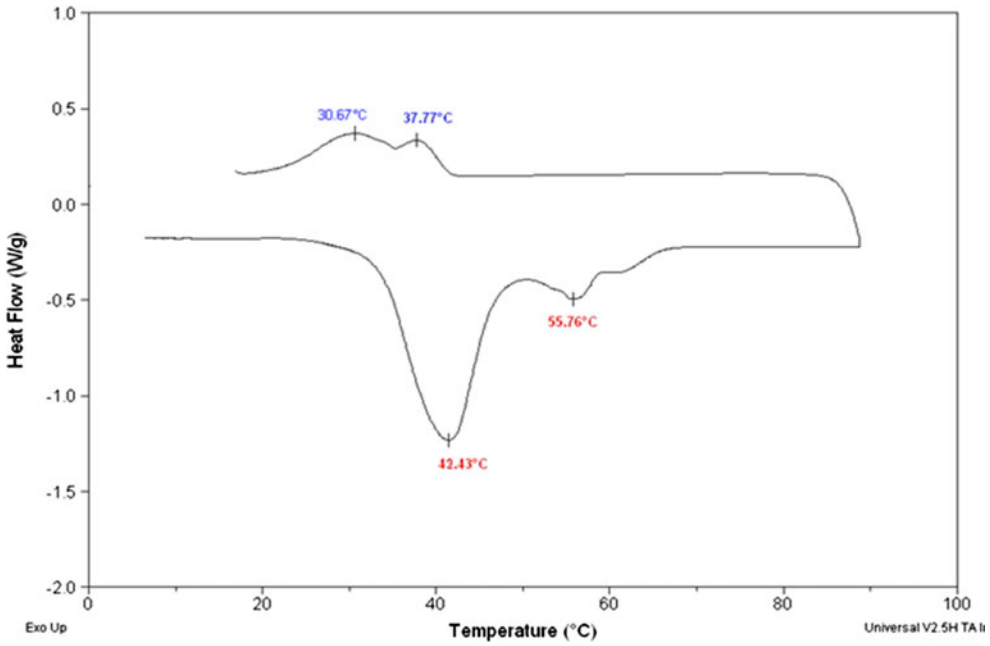


**Fig. 4** DSC thermogram of GMO-GMS (75:25 wt%) mixture showing a major melting peak around 42°C and crystallization peak at 37°C.

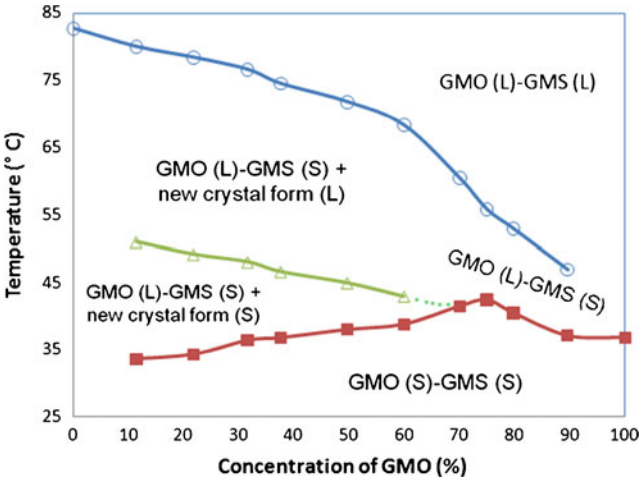


**Fig. 5** The phase diagram of GMO-GMS (0–100 wt%) matrices based on the peak melting temperature ($T_m$).

undergo several cycles of heating followed by cooling back to body temperature. To simulate this cycle, the samples were heated a second time and melting temperatures, $T_{m2}$, were observed. The values in Table I show that the critical melting point of the GMO-rich phase was again maximal at 75:25 wt% GMO-GMS, and that the values for $T_{m2}$ were only slightly lower than those observed during the first heat ($T_m$). Further, the $T_{m2}$ values for the α-form of GMS appeared to closely mirror the $T_m$ values found during the first heat. These results suggest that the melt characteristics of the matrix will not vary significantly as the system is heated and cooled repeatedly.

When deposited *in vivo* it is expected that the GMO-GMS matrix will absorb water, although the extent to which is unclear. The effect of hydration on the thermal response of the matrices containing a 2.5%, 8% and 24% (w/w) water content on GMO-GMS (1:3 weight ratio of lipids) were examined (thermograms shown in Supplementary Material). Compared to the anhydrous case, $T_m$ endotherms showed a shift to 74.5°C, 71.4°C and 57°C, upon the first heating cycle at 2.5%, 8% and 24% water content, respectively. Upon the second heating, the major endothermic peak was observed at 71°C, 65°C and 57°C for the 2.5%, 8%, and 24% samples, respectively.

Additives, such as free oleic acid, have been shown to modify the phase properties of GMO (reference). In separate experiments it was observed that the inclusion of 0.5% magnetic nanoparticles had no significant effect on the phase properties of the anhydrous 75:25 wt% GMO-GMS matrix as determined by DSC (data not shown). Since there is no free oleic acid in the nanoparticle preparation, it may be that the total amount of oleic acid bonded to the surface of the particles is insufficient to influence the ordering of the matrix lipids. These results are in agreement with those of Dilnawaz *et al*. (27). In a second set of control experiments, DSC thermograms were collected for anhydrous 75:25 wt% GMO-GMS matrices containing drug. No evidence of melting of crystalline NF (m.p. 172°C) in drug-containing GMO-GMS matrices was observed when subjected to multiple heat/cool cycles (data not shown). From these results, it may be concluded that there were no crystals of NF in the GMO-GMS matrices sufficiently large to be detected by DSC.

In summary, the GMO-rich phase in the 75:25 wt% mixture exhibited the appropriate $T_m$, $T_{m2}$ and $T_c$ temperatures as outlined in the model presented in Fig. 2 and were considered suitable for further study.

## Temperature-Dependent Nifedipine Release from GMO-GMS Matrices

The *in vitro* release of nifedipine (NF) from selected GMO-GMS matrices into ACSF was studied at 37°C and 42°C. Figure 6a shows the release of NF from GMO-GMS (25:75 wt%), Fig. 6b the release from GMO-GMS (50:50 wt%) and Fig. 6c the release from GMO-GMS (75:25 wt%). For all three matrices studied, the release of NF at 42°C was significantly higher than that at 37°C. For example, the GMO-GMS (75:25 wt%) matrix released about 35% of NF in 10 days at 37°C whereas 96% release was observed at 42°C within the same period of time. Further, and of most importance to this study, was the observation that the greatest difference in release between 37°C and 42°C was observed with a GMO-GMS (75:25 wt%) matrix (Fig. 6c). In a control experiment with the Float-A-Lyzer containing a nifedipine-saturated solution, transport equilibrium of the drug was reached within 2 h at 37°C. When the nifedipine concentration was reduced to 4 micrograms/mL, a value 30% of saturation, transport equilibrium was reached within 2.5 h. These rates of release were much faster than those observed from any of the GMO-GMS matrices and suggested that transport through the dialysis membrane was not the rate-determining step for matrix release. In a separate control experiment three dialysis membranes exposed simultaneously to a small volume of saturated solution of nifedipine in ACSF for 48 h at 37°C showed no evidence of solute binding.

## Remote Heating of the Monoglycerides Matrix Containing Magnetic Nanoparticles upon Exposure to an AMF

In the previous sections, the thermal and transport properties of GMO-GMS mixtures were evaluated and the results showed a temperature-dependent release of NF from the matrices. In this section, the ability to remotely heat the GMO-GMS matrices containing magnetic nanoparticles and exposed to an AMF as illustrated in Fig. 1 were examined.

Oleic acid-modified iron oxide magnetic nanoparticles (OA-$Fe_3O_4$) were utilized for heating of the GMO-GMS matrices upon exposure to AMF. The ability of OA-$Fe_3O_4$

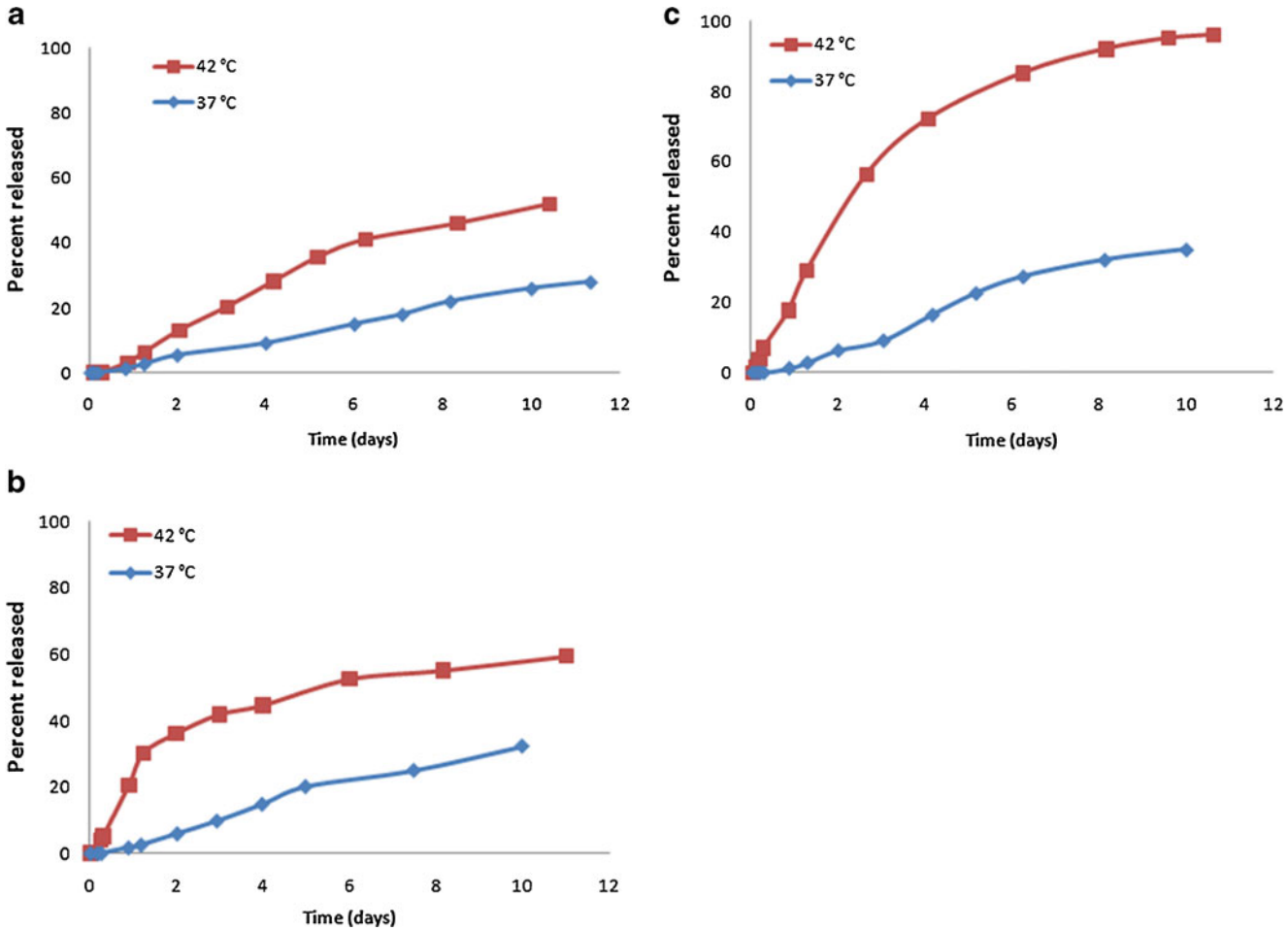


**Fig. 6** Temperature dependent *in vitro* release of nifedipine from the monoglycerides matrix at 37°C and 42°C (**a**) GMO-GMS (25:75 wt%), (**b**) GMO-GMS (50:50 wt%) and (**c**) GMO-GMS (75:25 wt%).

to induce a temperature change in the GMO-GMS matrices upon exposure to AMF was found to be dependent upon the monoglycerides composition. Figure 7a shows the rise in temperature of various GMO-GMS compositions containing 0.5% OA-$Fe_3O_4$ and exposed to AMF for 10 min. As the proportion of GMS increased, the matrix became more resistant to heating. The GMO-GMS (25:75 wt%) matrix containing 0.5% OA-$Fe_3O_4$ was heated to 38.9°C in 10 min, whereas the GMO-GMS (75:25 wt%) matrix was heated to 46.2°C during the same period of time. At present, it is not clear if the dependence of heating rate on composition is due to factors such as microscopic viscosity around the nanoparticles or due to heat capacity effects of the lipid matrix. No matter what the effect, it is clear that 10 min of exposure to AMF was able to induce rapid and reproducible temperature changes in the GMO-GMS matrices.

In order to optimize the amount of magnetic nanoparticles required to heat the system, GMO-GMS (50:50 wt%) matrix containing various concentrations 0.25–1.3% OA-$Fe_3O_4$ were exposed to AMF for 10 min. Figure 7b shows a concentration dependent heating capability of the OA-$Fe_3O_4$ exposed to AMF. A concentration of 1.3% OA-$Fe_3O_4$ heated the GMO-GMS (50:50 wt%) matrix to 63.4°C within 10 min of AMF exposure. On the other hand, 0.25% and 0.5% OA-$Fe_3O_4$ were able to heat the matrix to 41.6°C and 45.5°C, respectively. Based on the results, 0.5% OA-$Fe_3O_4$ was selected as an optimum amount needed to induce the phase transition of the matrix. Moreover, five minutes of exposure to AMF was sufficient to reach the required temperature .

## AMF-Triggered Nifedipine Release from GMO-GMS (75:25 wt%) Matrix Containing 0.5% OA-$Fe_3O_4$ Nanoparticles

NF release from a GMO-GMS (75:25 wt%) mixture containing 0.5% OA-$Fe_3O_4$ nanoparticles and NF and heated by AMF (Fig. 1) was examined. Samples of ASCF were analyzed for NF 2 h prior to and 2 h following a 5 min AMF exposure. The cumulative NF release from the GMO-GMS (75:25 wt%) matrix is plotted in Fig. 8. When AMF was applied (arrows in Fig. 8), the matrix underwent a phase

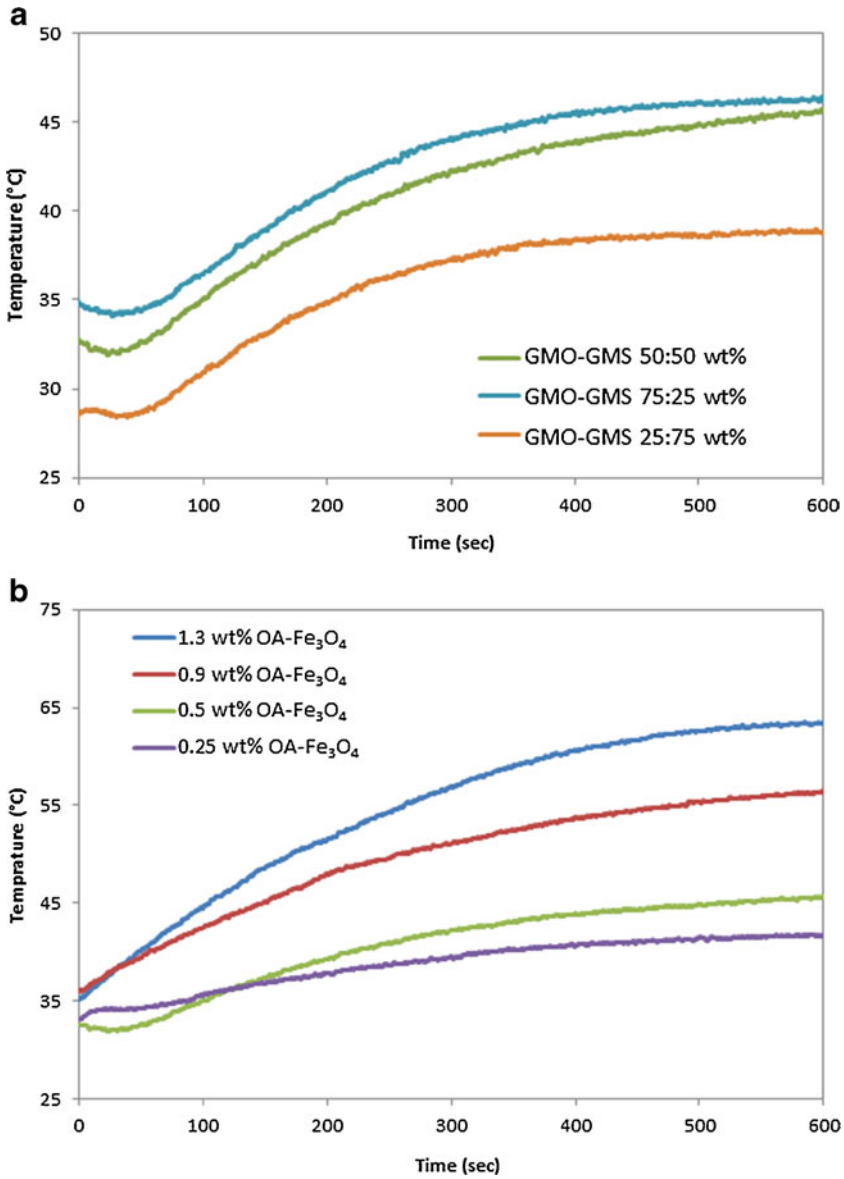


**Fig. 7** Remote heating of the monoglycerides matrix containing OA-$Fe_3O_4$ nanoparticles using AMF (**a**) Effect of the monoglycerides matrix composition on remote heating. The concentration of the OA-$Fe_3O_4$ nanoparticles was kept constant at 0.5 wt% and (**b**) Effect of the concentration of OA-$Fe_3O_4$ nanoparticles on heating of the monoglycerides matrix (GMO-GMS, 50:50 wt%).

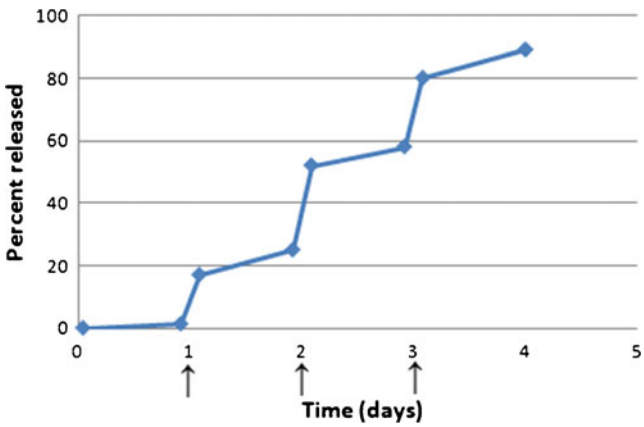


**Fig. 8** Alternating magnetic field (AMF) triggered *in vitro* release of nifedipine from GMO-GMS (75:25 wt%) matrix. The arrows indicate the exposure of the matrix to AMF for 5 minutes. Samples were analyzed 2 h before and after AMF exposure.

transition and a corresponding burst of NF release was observed. When the AMF is removed, NF release was reduced, putatively because the monoglycerides matrix recrystallized when the system returned to 37°C. Hence, release can be accelerated by the application of AMF and can result in a stepwise, on-demand release pattern.

## DISCUSSION

Lipid-based systems continue to be of great interest to the field of drug delivery and a variety of products for oral, parenteral and ophthalmic use are commercially available. Dispersions of lipids in water as emulsions, microemulsions, liposomes, and several cubic phases have garnered the most interest as drug delivery systems (28–31). Solubilization of poorly soluble

drugs and adaptation to modified release are two of several important advantages of lipid-based drug delivery systems (29,30). GMO has been studied for drug delivery as a depot matrix (32,33). As a dispersion in water GMO is able to form a variety of phase nanostructures, and thus solubilize a wide variety of molecules, both hydrophobic and hydrophilic (28,33). However, as a depot system, GMO seems to exhibit a limited ability to extend the release of the drug (29). In addition, the gel state of GMO often exhibits somewhat poor syringability, making for difficult parenteral administration (32,34).

In the present study, mixtures of GMO, GMS, and OA-$Fe_3O_4$ nanomagnets are examined *in vitro* as a matrix for the thermo-triggered release of a model hydrophobic drug. It is envisioned that a lipid matrix, contain a hydrophobic drug of interest and magnetic nanoparticles, would be inserted *in vivo*, such as in a cavity remaining after surgical resection of a tumor. The two biocompatible lipids individually have well-defined thermal properties and it is hypothesized that mixtures would provide the desired drug release properties in a rather narrow range of temperatures. The lipid matrix would melt upon application of an AMF, releasing the drug locally (24,27). In our studies, we have arbitrarily set this temperature to be no greater than 42°C, a value just above that of body temperature. Removing the AMF would permit the gel to solidify by returning to body temperature, greatly reducing the rate of drug release.

Ferromagnetic-assisted site-specific drug delivery and imaging have been the subject of extensive research (35–40). OA-$Fe_3O_4$ nanomagnets naturally resist movement in the rapidly alternating magnetic field within an inductive coil and the resulting friction produces hysteresis heating in addition to eddy current heating. Much of the work concerning nanomagnets has employed biocompatible thermo-responsive polymers as the drug delivery platform with only a few examples of application to lipid vesicles (41,42). OA-$Fe_3O_4$ nanoparticles employed in the current study exhibit a core-shell structure consisting of a mono- or multi-crystalline magnetic iron oxide and coated with a biocompatible fatty acid. The coating is essential to enhance miscibility of the OA-$Fe_3O_4$ nanoparticles in the monoglyceride matrix and to localize the magnetic nanoparticles in the long-chain non-polar region. Moreover, the process of coating alters the surface properties of the magnetic nanoparticles, reduces aggregation and improves colloidal stability (43).

Monoglycerides such as GMO are known to produce a wide-range of phase structures when in contact with water, including a variety of cubic phases. The influence of these phase properties on the characteristics of lipid-based drug delivery systems as dispersed nanoparticles has been frequently observed (28,29). The extent to which mixing of monoglycerides influences phase behavior and drug release is much less studied. In the current study, the DSC thermograms suggest the existence of two solid phases, one rich in GMO and the other rich in GMS. It is not yet possible to predict the phase properties when two or more lipids are mixed and, to our knowledge, there are no published studies examining the phase(s) present in GMO/GMS blends. It should be noted that DSC studies alone are not sufficient to provide a full picture of the extent of mixing of mixtures of GMO and GMS in the presence of water. Clogston *et al*. (44) have published a phase diagram of Myverol 18-99 K, a mixture of monoglycerides, including GMO (86% by weight) and GMS (7% by weight). These investigators concluded that their results were rather similar to the phase diagram reported by Qiu *et al*. (45) for pure GMO. In the current study, the concentrations of GMS relative to those of GMO are much higher than that of Myverol 18-99 K, so it is unlikely that a direct paralleling of properties would be expected. Returning to the phase diagram of Qiu (45), in the temperature range of 37 to 45°C at 8% water, GMO is in the $L_\alpha$ phase whereas at 24% water, the system is in La3d. In the presence of excess water, the results of Qiu indicated the system is Pn3m+water. The extent to which the GMO/GMS mixtures in the present study conform to the results of Qiu *et al*. are not known. Chong *et al*. (46) evaluated the effect of a variety of polyethylene oxide stearates ($PEO_x$-stearate) on the physical stability of cubic GMO nanodispersions. These authors report that short-chain PEOx-stearates exhibited increased internalization within the nanostructure, resulting in a change in the mesostructure from $V_2^D$ to $V_2^P$. Longer $PEO_x$-stearates were excluded from the internal structure. In the present study, GMS, which contains no polyethylene oxide, would likely have access to the internal structure of a putative cubic phase. As stated previously, the phase behavior of GMO-GMS mixtures has not been published, so the issue of the state of mixing of these two lipids is not yet settled. In a somewhat related study, Rodriguez, *et al*. (47) showed that GMO-GMS monolayer mixtures were poorly-miscible at the air-water interface. They observed "islands" of GMS dispersed within a "sea" of GMO.

While it may be argued that there is little direct applicability of monolayer studies to mixing in cubic phases, the results listed above do suggest that further studies of the mixing behavior of these two lipids are warranted. Better understanding of the mixing properties in the presence and absence of water would provide improved insight into the drug release characteristics and ultimately aid scientists in rapidly selecting optimal formulations.

## CONCLUSIONS

This work demonstrates the feasibility of controlled and triggered NF release from GMO-GMS (75:25 wt%) matrix

containing 0.5% oleic acid-modified $Fe_3O_4$ nanoparticles for the remotely heating using an alternating magnetic field as an external stimulus. The DSC and the *in vitro* NF release studies at 37°C and 42°C as well as the AMF triggered release support the hypothesis that appropriate blends of monoglycerides can be utilized for thermo-sensitive drug delivery system.

## ACKNOWLEDGMENTS AND DISCLOSURES

Abebe E. Mengesha and Robert J. Wydra contributed equally to this manuscript.

## REFERENCES

1. Lee ES, Oh KT, Kim D, Youn YS, Bae YH. Tumor pH-responsive flower-like micelles of poly(L-lactic acid)-b-poly (ethylene glycol)-b-poly(L-histidine). J Control Release. 2007;123(1): 19–26.
2. Abraham G, McCarroll J, Byrne F, Saricilar S, Kavallaris M, Bulmus V. Block co-polymer nanoparticles with degradable cross-linked core and low-molecular-weight PEG corona for anti-tumour drug delivery. J Biomater Sci Polym Ed. 2011;22(8):1001–22.
3. Chan AS, Chen CH, Huang CM, Hsieh MF. Regulation of particle morphology of pH-dependent poly(epsilon-caprolactone)-poly(gamma-glutamic acid) micellar nanoparticles to combat breast cancer cells. J Nanosci Nanotechnol. 2010;10(10):6283–97.
4. Yarmolenko PS, Zhao YL, Landon C, Spasojevic I, Yuan F, Needham D, *et al*. Comparative effects of thermosensitive doxorubicin-containing liposomes and hyperthermia in human and murine tumours. Int J Hyperth. 2010;26(5):485–98.
5. Hua MY, Liu HL, Yang HW, Chen PY, Tsai RY, Huang CY, *et al*. The effectiveness of a magnetic nanoparticle-based delivery system for BCNU in the treatment of gliomas. Biomaterials. 2011;32(2):516–27.
6. Misra RDK. Core-shell magnetic nanoparticle carrier for targeted drug delivery: challenges and design. Mater Technol. 2010;25(3–4): 118–26.
7. Robinson I, Alexander C, Tung LD, Fernig DG, Thanh NTK. Fabrication of water-soluble magnetic nanoparticles by ligand-exchange with thermo-responsive polymers. J Magn Magn Mater. 2009;321(10):1421–3.
8. Satarkar NS, Meenach SA, Anderson KW, Hilt JZ. Remote actuation of hydrogel nanocomposites: heating analysis, modeling, and simulations. AIChE J. 2011;57(4):852–60.
9. Satarkar NS, Hilt JZ. Magnetic hydrogel nanocomposites for remote controlled pulsatile drug release. J Control Release. 2008;130(3): 246–51.
10. Liu Y, Paliwal S, Bankiewicz KS, Bringas JR, Heart G, Mitragotri S, *et al*. Ultrasound-enhanced drug transport and distribution in the brain. Aaps Pharmscitech. 2010;11(3):1005–17.
11. De Geest BG, Skirtach AG, Mamedov AA, Antipov AA, Kotov NA, De Smedt SC, *et al*. Ultrasound-triggered release from multilayered capsules. Small. 2007;3(5):804–8.
12. Chen PY, Liu HL, Hua MY, Yang HW, Huang CY, Chu PC, *et al*. Novel magnetic/ultrasound focusing system enhances nanoparticle drug delivery for glioma treatment. Neuro-Oncology. 2010;12(10): 1050–60.
13. Meng H, Hu JL. A brief review of stimulus-active polymers responsive to thermal, light, magnetic, electric, and water/solvent stimuli. J Intell Mater Syst Struct. 2010;21(9):859–85.
14. Meenach SA, Otu CG, Anderson KW, Hilt JZ. Controlled synergistic delivery of paclitaxel and heat from poly(beta-amino ester)/iron oxide-based hydrogel nanocomposites. Int J Pharm. 2012;427(2):177–84.
15. Grayson SM, Godbey WT. The role of macromolecular architecture in passively targeted polymeric carriers for drug and gene delivery. J Drug Target. 2008;16(5):329–56.
16. Fong WK, Hanley T, Boyd BJ. Stimuli responsive liquid crystals provide 'on-demand' drug delivery in vitro and in vivo. J Control Release. 2009;135(3):218–26.
17. Kono K, Nakashima S, Kokuryo D, Aoki I, Shimomoto H, Aoshima S, *et al*. Multi-functional liposomes having temperature-triggered release and magnetic resonance imaging for tumor-specific chemotherapy. Biomaterials. 2011;32(5):1387–95.
18. Gan L, Han S, Shen JQ, Zhu JB, Zhu CL, Zhang XX, *et al*. Self-assembled liquid crystalline nanoparticles as a novel ophthalmic delivery system for dexamethasone: improving preocular retention and ocular bioavailability. Int J Pharm. 2010;396(1–2):179–87.
19. Lai J, Chen JM, Lu Y, Sun J, Hu FQ, Yin ZN, *et al*. Glyceryl monooleate/poloxamer 407 cubic nanoparticles as oral drug delivery systems: I. In vitro evaluation and enhanced oral bioavailability of the poorly water-soluble drug simvastatin. AAPS PharmSciTech. 2009;10(3):960–6.
20. Sato K. Crystallization behaviour of fats and lipids—a review. Chem Eng Sci. 2001;56:2255–65.
21. Batte HD, Wright AJ, Rush JW, Idziak SHJ, Marangoni AG. Phase behavior, stability, and mesomorphism of monostearin-oil-water gels. Food Biophys. 2007;2:29–37.
22. Biltonen RL, Lichtenberg D. The use of differential scanning calorimetry as a tool to characterize liposome preparations. Chem Phys Lipids. 1993;64:128–42.
23. Heertje I, Roijers EC, Hendrickx HACM. Liquid crystalline phases in the structuring of food products. Food Sci Technol. 1998;31:387–96.
24. Laquintana V, Trapani A, Denora N, Wang F, Gallo J, Trapani. New strategies to deliver anticancer drugs to brain tumors. Expert Opin Drug Deliv. 2009;6:1017–32.
25. Frimpong RA, Hilt JZ. Poly(n-isopropylacrylamide)-based hydrogel coatings on magnetite nanoparticles via atom transfer radical polymerization. Nanotechnology. 2008;19(17):0957–4484.
26. Vereecken J, Meeussen W, Foubert I, Lesaffer A, Wouters J, Dewettinck K. Comparing the crystallization and polymorphic behaviour of saturated and unsaturated monoglycerides. Food Res Int. 2009;42(10):1415–25.
27. Dilnaqaz F, Singh A, Mohanty C, Sahoo S. Dual drug loaded superparamagnetic iron oxide nanoparticles for targeted cancer therapy. Biomaterials. 2010;31:3694–706.
28. Mulet X, Boyd B, Drummond C. Advances in drug delivery and medical imaging using colloidal lyotropic liquid crystalline dispersions. J Colloid Interface Sci. 2013;393:1–20.
29. Nguye T-H, Hanley T, Porter C, Boyd B. Nanostructured liquid crystalline particles provide long duration sustained-release effect for a poorly water soluble drug after oral administration. J Control Release. 2011;153:180–6.
30. Date A, Nagarsenker M. Parenteral microemulsions: an overview. Int J Pharm. 2008;355:19–30.
31. Heurtault B, Saulnier P, Rech B, Proust J-E, Benoit J-P. Physico-chemical stability of colloidal lipid particles. Biogeosciences. 2003;24: 4283–300.
32. Ganem-Quintanar A, Quintanar-Guerrero D, Buri P. Monoolein: a review of the pharmaceutical applications. Drug Dev Ind Pharm. 2000;26:809–21.
33. Kulkarni C, Wachter W, Iglesias-Salto G, Engelskirchen S, Ahualli S. Monoolein: a magic lipid. Phys Chem Chem Phys. 2011;13:3004–21.
34. Sein A, Verheij J, Agterof W. Rheological characterization, crystallization, and gellation behavior of monoglyceride gels. J Colloid Interface Sci. 2002;249:412–22.

35. Hawkins AM, Satarkar NS, Hilt JZ. Nanocomposite degradable hydrogels: demonstration of remote controlled degradation and drug release. Pharm Res. 2009;26(3):667–73.
36. Zhu L, Huo Z, Wang L, Tong X, Xiao Y, Ni K. Targeted delivery of methotrexate to skeletal muscular tissue by thermosensitive magnetoliposomes. Int J Pharm. 2009;370(1–2):136–43.
37. Talelli M, Rijcken CJ, Lammers T, Seevinck PR, Storm G, van Nostrum CF, *et al*. Superparamagnetic iron oxide nanoparticles encapsulated in biodegradable thermosensitive polymeric micelles: toward a targeted nanomedicine suitable for image-guided drug delivery. Langmuir. 2009;25:2060–7.
38. Cheng R, Meng F, Deng C, Klok H-A, Zhong Z. Dual and multi-stimuli responsive polymer nanoparticles for programmed site-specific drug delivery. Biogeosciences. 2013;34:3647–57.
39. Abutaltelleh SR, Spain SG, Aylott JW, Chan WC, Garnett MC, Alexander C. Thermoresponsive polymer colloids for drug delivery and cancer therapy. Macromol Biosci. 2011;11:1722–9.
40. Kumar CSSR, Mohammad F. Magnetic nanomaterials for hyperthermia-based therapy and controlled drug delivery. Adv Drug Deliv Rev. 2011;63:789–808.
41. Nappini S, Al-Kayal T, Berti D, Bengt N, Baglioni P. Magnetically triggered release from giant unilamellar vesicles: visualization by means of confocal microscopy. J Phys Chem Lett. 2011;2:713–8.
42. Bolfarini G, Siqueira-Moura M, Demets J, Morais P, Tedesco A. In vitro evaluation of combined hyperthermia and photodynamic effects using magnetoliposomes loaded with cucurbituril zinc phthalocyanine complex on melanoma. J Photochem Photobiol B. 2012;115:1–4.
43. Petri-Fink A, Steitz B, Finka A, Salaklang J, Hofmann H. Effect of cell media on polymer coated superparamagnetic iron oxide nanoparticles (SPIONs): colloidal stability, cytotoxicity, and cellular uptake studies. Eur J Pharm Biopharm. 2008;68:129–37.
44. Clogston J, Rathman J, Tomasko D, Walker H, Caffrey M. Phase behavior of a monoacylglycerol: (Myverol 18-99K)/water system. Chem Phys Lipids. 2000;107:191–9.
45. Qui H, Caffrey M. The phase diagram of the monoolein/water system: metastability and equilibrium aspects. Biogeosciences. 2000;21:223–34.
46. Chong JYT, Mulet X, Waddington LJ, Boyd BJ, Drummond CJ. High-throughput discovery of novel steric stabilizers for cubic lyotropic liquid crystal nanoparticle dispersions. Langmuir. 2012;28:9223–32.
47. Rodriguez-Nino MR, Wilde PJ, Clark DC, Rodriquez-Patino JM. Surface rheological properties of monostearin and monoolein films spread on the air-aqueous phase interface. Ind Eng Chem Res. 1996;35:4449–53.